E3S Web of Conferences **672**, 07027 (2025)
ROOMVENT 2024
https://doi.org/10.1051/e3sconf/202567207027

Effect of solar shielding and thermal insulation for comfortable energy-efficient residential building in mild climate

Tomoka Kawamura[1*], *Yasuhiro* Shimazaki[1], *Masaki* Tajima[1] and *Atsuo* Shimizu[2]

[1] Toyohashi University of Technology, Department of Architecture and Civil Engineering, Toyohashi, 4418580, Japan
[2] INOAC Corporation, Nagoya, 4500003, Japan

Abstract. In this study, we conducted a field measurement in a highly airtight and highly insulated house in a mild climate in Japan. By installing solar shielding on windows, the temperature of the interior window surface decrease, and create longer time lag. In addition, heat flux from the window surface was decrease, that of the other parts was increased. The CFD analysis showed that the heat flux from the attic could be reduced by increasing roof insulation and ventilation through the eaves.

1 Introduction

In Japan, the energy consumption in the household sector is increasing annually. In the building sector, aiming to achieve targets for the reduction of greenhouse gas emissions, ensuring the energy efficiency performance of ZEH and ZEB standards is to be aimed for newly built houses or buildings from 2030 onwards. Countermeasures have been taken to improve the efficiency of hot-water supply and ventilation systems in houses, save energy in home appliances, use LED lighting fixtures, and increase the thermal insulation of buildings. As a result of these measures, the annual energy consumption in general areas under Japan's energy conservation standards has been decreasing, from approximately 9000 kWh/year to less than 7000 kWh/year in approximately 10 years [1]. Highly airtight and insulated houses are becoming more common, with the aim of reducing the heating load and improving comfort; however, an increase in the cooling load has been pointed out regarding application to warmer climates [2,3]. In Japan, in addition to conventional measures, thermal insulation measures for the external skin are also being taken against the background of the Building Energy Conservation Law. As a solar shading measure for window surfaces, it has been shown that a solar shield film on window surfaces can reduce the heat load from windows, thereby reducing the cooling load and energy consumption of the entire building [4].

In this study, the thermal environment of a highly airtight and insulated house in summer was investigated. Also, the indoor and outdoor temperatures and solar radiation were measured and compared before and after installing solar shielding films on the second floor openings. Based on the measured results, countermeasures to improve the indoor thermal environment were investigated using CFD analysis.

2 Field measurements

2.1 Outline of a target building

A target house was located in Anjo City, Japan known for its mild climate, and was a highly airtight and highly

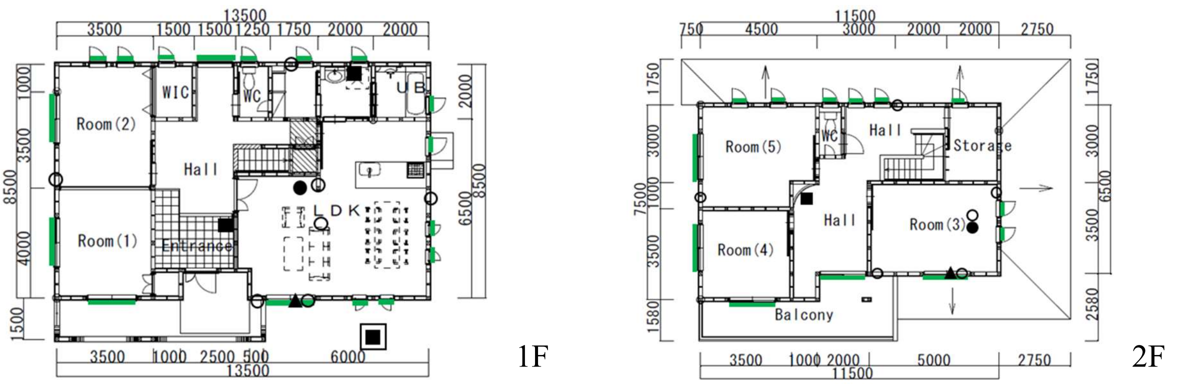

○ Surface temperature ■ Air temperature and relative humidity ▲ Solar radiation
● Globe temperature, air temperature and relative humidity ▬ Solar shielding □ Instrument shelter
Fig. 1. Installation locations of measuring instruments and films

* Tomoka Kawamura: kawamura.tomoka.zw@tut.jp

insulated with a triple-glazed window system. It is a two-story building with a total floor area of 191.5 m^2 and a building area of 126.0 m^2. The first floor had two air-conditioning units, one in the entrance hall and one in the living/dining/kitchen area, whereas the second floor had one unit. The house also had an overall air-conditioning system. Typically, one or two staff members occupied the house during weekdays as it served as a model house. Solar shielding films was installed on all first-floor window surfaces in August 2022, and on all second-floor window surfaces in April 2023, to prevent heat gain through the openings. The solar shielding had a solar transmittance of 0.421 and a reflectance of 0.145.

We conducted measurements on power consumption and thermal environmental variables, including air temperature and solar radiation at windows. Fig. 1 shows the installation locations of measuring instruments and films.

2.2 Evaluation methodology

In this study, the thermal environment of the second floor Room (3) was evaluated for the summer periods of before (2022) and after (2023) installing the solar shielding films. The radiation environment was verified by using equation (1) to estimate the mean radiant temperature, MRT based on the glove temperature θ_g [°C], room ait temperature θ_r [°C] and air velocity v [m/s]. The heat gain q_i [W/m^2] from the ceiling, walls, windows and floor was calculated using equation (2), where θ_{si} [°C] is the interior surface temperature of each component and α_i [W/(m^2·K)] is the total interior heat transfer coefficient. i indicates internal walls, ceiling, south wall, west wall, and floor.

$$MRT \fallingdotseq \theta_g + 2.35\sqrt{v}(\theta_g - \theta_r) \quad (1)$$

$$q_i = \alpha_i(\theta_{si} - \theta_r) \quad (2)$$

2.3 Result and discussion

In order to compare the indoor thermal environment with and without the solar radiation shielding film, the following days (11/8/2022 and 25/8/2023) were selected: the maximum value of total solar radiation was above 1000 W/m^2, the maximum outdoor temperature was above 30 °C and the air conditioning set temperature was 26 °C. Fig. 2 shows outdoor and indoor air temperature, the outside and inside window temperatures, and solar radiation of the west-facing

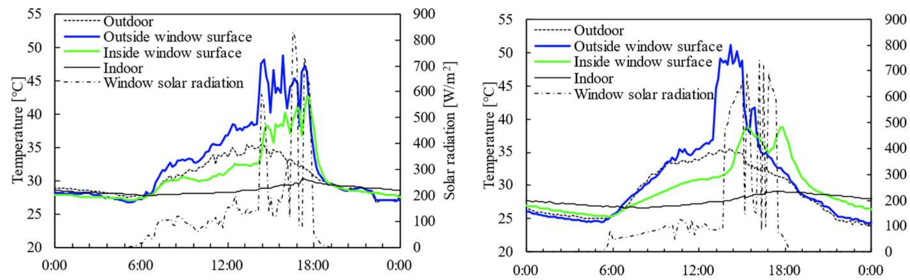

(a) 2022/8/11 (b) 2023/8/26

Fig. 2. Window surface temperatures and window solar radiation

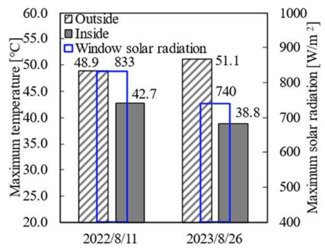

Fig. 3. Maximum surface temperature and solar radiation on window

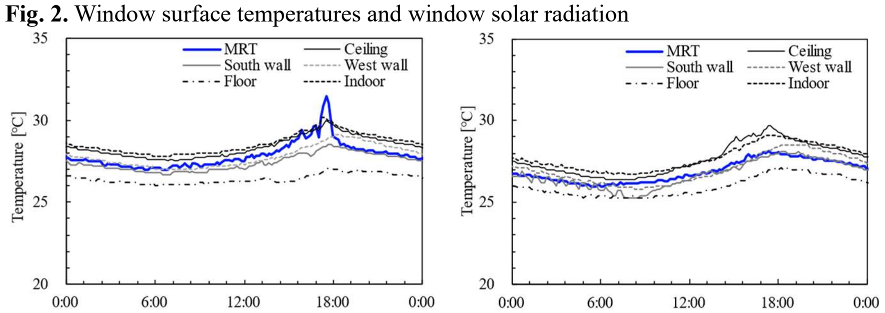

(a) 2022/8/11 (b) 2023/8/26

Fig.4. MRT and indoor surface temperature

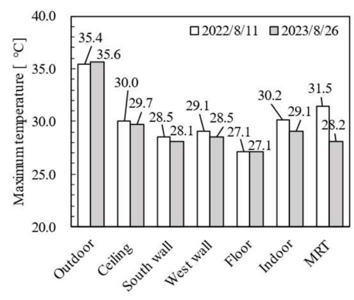

Fig. 5. Maximum temperature

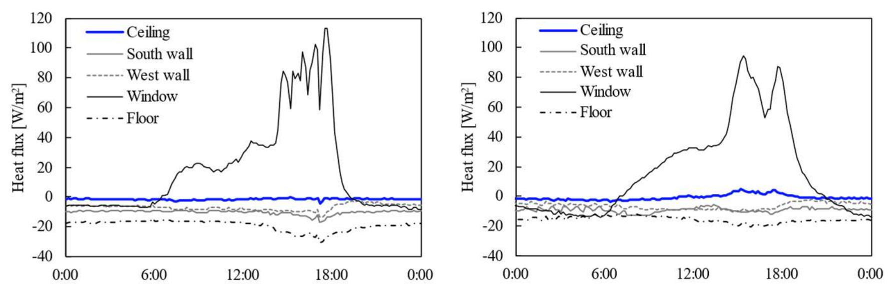

(a) 2022/8/11 (b) 2023/8/26

Fig. 6. Heat fluxes to the room

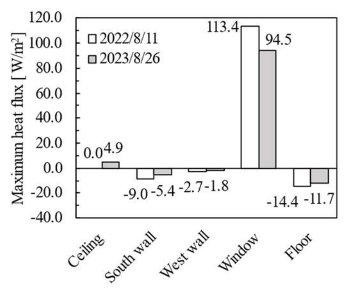

Fig. 7. Maximum heat flux

window. Fig. 3 shows these maximum values. As the outdoor temperature and the solar radiation increased, the outside window surface temperature increased. The window surface temperature was higher on the outside than on the inside, with a difference of 6.2 °C in 2022 and 12.3 °C in 2023. Table 1 presents the peak times and time lags of the surface window temperatures, both on the outside and inside. In 2023, the time lag was 1 hour and 40 minutes, which is 1 hour and 50 minutes longer than in 2022. The windows reduced heat transfer into the room, likely due to the increased thermal inertia caused by the installation of the film.

Table 1. Peak time of the window and time lag (JST)

	11/8/2022	26/8/2023
Outside	3:50 p.m.	2:10 p.m.
Inside	5:30 p.m.	5:40 p.m.
Time lag	1:40	3:30

Fig. 4 shows the *MRT* and the indoor surface temperatures at each part, and Fig. 5 shows its maximum value. The surface temperatures varied between 1 and 3 °C over the course of the day. In 2022, the maximum *MRT* was 1.3 °C higher than the indoor temperature, whereas in 2023, it was 0.9 °C lower. The maximum ceiling temperature was 2.9 °C higher than the floor in 2022 and 2.6 °C higher in 2023. And it was 1.5 °C lower than the *MRT* in 2022 and 1.5 °C higher in 2023. It describes a vertical temperature difference that causes thermal discomfort in the room, and the ceiling affects increasing the amount of heat radiation received by the human body. The maximum outdoor air temperature in 2023 was 0.2 °C higher than in 2022, whereas the indoor temperature was 1.1 °C lower and the *MRT* was 3.3 °C lower.

Fig. 6 displays the heat flux q_i from each indoor site, and Fig. 7 shows the maximum values. The heat gain from window surfaces increased between 2:00 pm and 6:00 pm, while the heat gain from walls and the floor decreased. The maximum heat flux from windows was 18.9 W/m^2 lower in 2023 than in 2022, while the heat flux from other parts of the building was higher in 2023, and 4.9 W/m^2 higher on the ceiling surface. Window surfaces are transparent components and have a significant heat load on the room. In 2023, the heat gain from the windows was reduced, and the *MRT* was lower. This reduction was achieved by installing solar radiation shielding film. Additionally, the decrease in heat gain from the windows led to an increase in heat gain from other parts of the building. Based on these results, it is necessary to take countermeasures for the ceiling in order to improve thermal comfort. This is because the ceiling value of the maximum temperature after film application exceeds *MRT* and the heat gain is positive.

3 Suggestions for improving indoor thermal environment

In Chapter 2, it was considered necessary to take countermeasures for the ceiling surface, in order to improve the thermal environment on the second floor. It was considered that improving the thermal environment in the attic contributes to decreasing the ceiling surface temperature. Therefore, the thermal environment in the attic was simulated using CFD analysis, and countermeasures to improve the thermal environment were proposed.

3.1 Outlines of CFD analysis

The CFD analysis assumes 26/8/2023, which was selected as the representative date in Chapter 2. The analysis model had a flat roof of equal volume to the experimental house, with the second floor 1.0 m below the ceiling. The interior temperature of the second floor was fixed at 26 °C and there were no internal walls or partitions. Table 2 shows analysis conditions and Fig. 8 shows analysis model. Ten ventilation holes (910 × 600 mm) were provided at the eaves, each with an air flow rate Q_{max}, Q_{min} [m^3/s] calculated by Equation (3), where α [−] is the flow coefficient, A [m^2] is the opening area behind the eaves, C [−] is the wind pressure coefficient, and v [m/s] is the external air velocity. The wind pressure coefficient is the value for the wall beneath the eaves (C_1 = 0.8, C_2 = -0.4) as specified in the Japanese Building Standard Law Enforcement, and the external air velocity is the average value of 1.5 m/s during June to September from weather data from Okazaki City [6], which is close to Anjo City where the subject house is located. The flow rates were calculated using α_{min} 0.07, assuming that the peg board was currently installed, and α_{max} 0.78, which assumed the mesh material, and were used as Q_{1min} and Q_{1max}, respectively.

$$Q = \alpha A \sqrt{(C_1 - C_2)v^2} \quad (3)$$

Table 2. Analysis conditions

Turbulence model	CHEN-KIM k-ε
Object size (Domain size)	13×8×1.8 m (20×10×3 m)
Time dependence	Steady
Global solar radiation	957 W/m^2 (Design value in Tokyo [5])
Ambient temperature	35.1 °C
Room temperature	26 °C Fixed
SAT	(A)68.6 (B)43.7 (C)68.6 °C
Insulation thickness	(A)100 (B)100 (C)200 mm
Roof solar absorption	(A)0.9 (B)0.3 (C)0.9

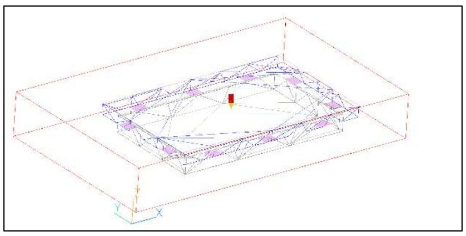

Fig. 8. Analysis model

Six scenarios were considered varying the flow rate at the eaves for (A) Baseline, which assumes the current subject house, and the two improved cases (B) High reflectivity and (C) High insulation. (B) assumes a solar absorptance for the roof of 0.3 and (C) assumes an insulation thickness above the ceiling of 200 mm.

3.2 Result and discussion

Table 3 shows the results mean values of the CFD analysis and the measured values, while Fig. 8 shows the temperature distribution. The mean attic air temperature difference between the measured value and (A) Q_{1min} assumed current conditions is only 2.3 °C. The lowest temperature, (B) Q_{1max} is 11.3 °C lower than (A) Q_{1min}. The attic temperature was lower when the flow rate was higher in Q_{1max} compared to Q_{1min}. The mean inside surface temperature of the ceiling had a difference of less than 0.1°C between the cases.

In order to evaluate the impact on the indoor thermal environment, the heat load through the attic to the room $|Q_1|$ [W] was calculated by equation (4), where U [W/m^2] is heat transfer coefficient of the ceiling, A_c [m^2] is the ceiling area, θ_a [°C] is attic air temperature, and θ_r [°C] is room air temperature. The difference between measured value and (A) Q_{1min} was 15.0 W. This is because the room air temperature is fixed. In case of this study which is based on the comparison in each scenario, this difference can be ignored. The heat load was lower in the order of (C), (B), and (A), and it was also lower in the case Q_{1max}, whose flow rate was higher, compared to Q_{1min}. The minimum heat load, (C) Q_{1min}, decreased by 44.9 W to (A) Q_{1max}. The difference of heat load is affected by the temperature difference between the attic air and the room air. As the room air temperature was fixed, the high values of the attic temperature led to the high heat loads. (C) had the smallest heat load from the attic, suggesting that the thermal conductivity of the insulation above the ceiling was small and heat from the attic was not transferred to the ceiling surface. The attic temperature was low and the heat load from the attic to the room was also low in the Q_{1max} scenario, suggesting that cooler outdoor air flows in while the warm attic air is exhausted outside. Therefore, increasing attic ventilation is an effective way of reducing heat loads in summer, as the temperature of the outside air is lower than that of the attic air.

Table 2. Results of CFD analysis

Case		Attic air [°C]	Ceiling surface [°C]	Heat load [W]
Q_{1min}	A	47.8	26.5	73.5
	B	38.3	26.5	41.3
	C	45.1	26.5	32.9
Q_{1max}	A	41.0	26.4	50.4
	B	36.5	26.5	35.3
	C	42.6	26.5	28.5
Measured		45.6	28.2	60.6

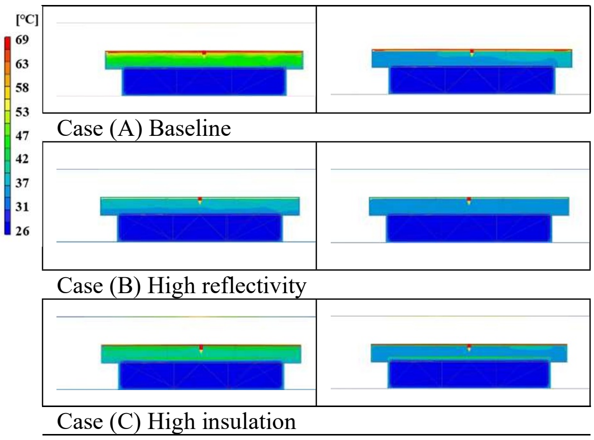

Fig. 5. Air temperature distributions (Left: Q_{1min} Right: Q_{1max})

$$|Q_1| = UA_c(\theta_a - \theta_r) \tag{4}$$

4 Conclusion

We conducted a field measurement in a highly airtight and highly insulated house with (2022) and without (2023) solar shielding film installed on windows, in a mild climate in Japan. The study was conducted during summer, and the following results were obtained:

- The installation of the film resulted in a decrease in the temperature of the interior window surface. Additionally, it increased the thermal inertia of the window and caused a time lag of 1 hour and 50 minutes between the outdoor and indoor sides.
- The temperature of the ceiling was higher than that of the *MRT* and the floor, creating a vertical temperature difference in the room, which was considered to worsen the radiation environment for the human body.
- The maximum heat flux from the window surface was 26.1 W/m^2 lower in 2023 than that in 2022. In contrast, the maximum heat flux from the other parts slightly greater.
- The CFD analysis showed that increasing roof insulation and ventilation through the attic could reduce the amount of heat loads from the attic to the room by 44.9 W.

References

1. M. Oota et al., *Analysis of HEMS data in a detached house (Part1)*, Journal of Environmental Engineering (Transactions of AIJ), 85(772), 495-502 (2020)
2. K. Ono et al., *Effects of Thermal Insulation and Shading on Air Conditioning Load of Dwelling in Mild Climate*, J. Human and Living Environment, 4(1), 52-60 (1996)
3. T. Miura et al., *Study on Performances of Highly Insulated Airtight Houses in Seasonal Hot and Humid Zones*, The Society of Heating, Air-Conditioning Sanitary Engineers of Japan, 121-124 (2011)
4. T. Kasashima, et al., *Investigation on heat-flow and energy consumption by solar shielding at the openings*, IBPSA Building Simulation 2023, ID1239 6 pages (2023)
5. Air-Conditioning Sanitary Engineers of Japan, Handbook of Air-Conditioning Sanitary Engineers, 14 (2010)
6. IBECs, Meteorological data, https://www.jjj-design.org/asset/img/jjj_archive/2017/05/23aichi.pdf